

Spline Implementation of Generalized Gradient Approximations to the Exchange-Correlation Functional and Study of the Sensitivity of Density Functional Accuracy to Localized Domains of the Reduced Density Gradient

Roberto Peverati and Donald G. Truhlar*

Department of Chemistry and Supercomputing Institute, University of Minnesota, Minneapolis, Minnesota 55455, United States

ABSTRACT: We present a natural cubic spline implementation of the exchange enhancement factor as a function of the reduced density gradient, and we demonstrate its performance by replicating the results of common GGA functionals. We also investigate the effect on the accuracy of various calculated properties of changing the shape of the exchange enhancement factor and an analogous factor for correlation. The properties considered are main group atomization energies, ionization potentials, electron affinities, proton affinities, alkyl bond dissociation energies, difficult hydrocarbon cases, barrier heights for chemical reactions, noncovalent interactions, atomic energies, metal bond energies, and main group bond lengths.

1. INTRODUCTION

The success of Kohn–Sham density functional theory rests on the accuracy with which one approximates the exchange-correlation functional, usually just called the density functional.¹ Although modern density functionals often depend on a number of variables including the density, the density gradient, the Laplacian of the density, the orbital-dependent Hartree–Fock energy, and the orbital-dependent kinetic energy density, they are almost all built by adding ingredients to the generalized gradient approximation (GGA), in which the density functional depends on just the density and the density gradient.

In the context of generalized gradient approximations, the exchange functional is usually expressed in terms of the electron density, ρ , and its gradient, $\nabla\rho$, as a simple product of the local spin density approximation (LSDA) and an enhancement factor:

$$E_x^{\text{GGA}} = \int d^3r \rho \varepsilon_x^{\text{LSDA}}(\rho) F_x^{\text{GGA}}(s) \quad (1)$$

where (all equations are in Hartree atomic units)

$$\varepsilon_x^{\text{LSDA}} = -(3/4)(3/\pi)^{1/3} \rho^{1/3} \quad (2)$$

is the exchange energy density per particle for a uniform electron gas (UEG), F_x^{GGA} is the enhancement factor, and

$$s = |\nabla\rho|/[2(3\pi^2)^{1/3} \rho^{4/3}] \quad (3)$$

is the variable called the dimensionless reduced gradient, defined on the interval $s \in [0, \infty)$.

All of the formulas are presented for a closed-shell system, where we can dispense with the spin components; the extension to open shells is standard and summarized in the Appendix. The approximation called LSDA here reduces to the local density approximation (LDA) for closed-shell Slater determinants with all orbitals doubly occupied, but we call it LSDA in all of our publications because that is the more general case, of which LDA

is a special case, and it would be confusing to use both names for this kind of functional (the description of all functionals becomes simpler for closed-shell systems).

As suggested by Becke,² it is convenient to perform a change of variable from the variable s to a new finite variable

$$u_\gamma = \frac{\gamma s^2}{1 + \gamma s^2}, u_\gamma \in [0, 1] \quad (4)$$

and to define the enhancement factor as a function of the new variable, where γ is a constant. We will use a special case u of this variable with $\gamma = 1$:

$$u = \frac{s^2}{1 + s^2} \quad (5)$$

and eq 1 can be expressed in the new variable as

$$E_x^{\text{GGA}} = \int d^3r \rho \varepsilon_x^{\text{LSDA}}(\rho) F_x^{\text{GGA}}(u) \quad (6)$$

Then, the exchange energy is completely determined by the shape of the curve $F(u)$ in the region $u \in [0, 1]$.

The shape of $F_x^{\text{GGA}}(s)$ or $F_x^{\text{GGA}}(u)$ can be expressed in many different ways, the more common ones being simple functions of s (as in the PBE,³ RPBE,⁴ and B88⁵ functionals), or polynomial expansions (as in the B97² and SOGGA11⁶ functional), with coefficients determined by some combination of physical constraints and fitting to experimental or theoretical data or both. In general the flexibility of $F(s)$ or equivalently $F(u)$ is limited by the chosen functional form. Similar but more complicated considerations apply to the correlation functional.

An alternate way to define a continuous and differentiable $F_x^{\text{GGA}}(u)$ curve is to fix some points (knots) and then use a spline to interpolate them. If a cubic spline is used, then by construction

Received: September 3, 2011

Published: October 27, 2011

it provides continuous first and second derivatives. Higher-order splines or splines under tension can also be used. An advantage of using splines to represent $F_x^{\text{GGA}}(u)$ is that the exchange-correlation functional is not constrained by preconceptions about the functional form.

The present article has two parts. In the first part, we show that the spline representation of density functionals is not just a theoretical possibility but that it actually works well in practice. In the second part, we use a spline implementation of exchange and correlation functionals to show the sensitivity of the accuracy of several properties to specific regions of u (and therefore also, by eq 5, to specific regions of s).

2. DATABASE

The database used in this article comprises 12 subsets (smaller databases) corresponding to various chemical properties. All subsets are the same as used in our recent SOGGA11 paper,⁶ where they were mainly based on previous work.^{7–25} The properties of the subsets are as follows: main-group atomization energies (MGAE109/05),¹² ionization potentials (IP13/03),^{10,12–14} electron affinities (EA13/03),^{10,12–14} proton affinities (PA8/06),²² alkyl bond dissociation energies (ABDE12),^{6,12,15,16} difficult hydrocarbon cases (HC7/11),^{6,23,24} barrier heights (HTBH38/08 and NHTBH38/08),^{12,17,18,25} noncovalent interactions (NCCE31/05),^{11,13,21,24} atomic energies (AE17),⁸ metal bond energies (SRMBE12 and MRMBE5),^{6,19,20} and main-group bond lengths (MGBL19).^{9,15}

The database is composed of 303 Born–Oppenheimer energies (that is, electronic energies including nuclear repulsion) or relative energies and 19 bond lengths. For example, for bond energies, we use equilibrium dissociation energies (D_e), not ground-vibrational-state dissociation energies (D_0) or bond enthalpies at finite temperature; the equilibrium dissociation energy is the difference between the Born–Oppenheimer energy at the dissociation limit and the equilibrium geometry. Relative energy data (including dissociation energies, barrier heights, overall energies of reactions, ionization potentials, van der Waals binding energies, etc.) require more than one single-point energy calculation, and therefore the total number of single-point calculations performed for the energetic part of the database is 350.

Geometries are the same as used previously.⁶

Next, we give more details of the database subsets.

2.1. Main Group Atomization Energies (MGAE109/05).

The MGAE109/05 database⁶ consists of 109 atomization energies (AEs) for main-group compounds. We always give the mean errors in atomization energies on a per bond basis because that makes comparison between different test sets more portable. To make it possible for readers to convert to the mean unsigned error per molecule, we always compute the mean errors in atomization energies by computing the mean error per molecule and then dividing by the average number of bonds per molecule in the test set; the latter value is 4.71 for MGAE109/05. Geometries for all molecules in this database are obtained with the QCISD/MG3 method.^{7,26,27}

2.2. Ionization Potentials, Electron Affinities, and Proton Affinities (IP13/03, EA13/03, PA8/06). The zero-point-exclusive adiabatic ionization potential (IP) and electron affinity (EA) test sets are called IP13/03 and EA13/03, respectively, and they have been explained and employed in our previous papers.^{10,12–14} Geometries for both neutral and ionic species in

the IP13/03 and EA13/03 databases are optimized separately by QCISD/MG3,^{9,21} i.e., these are adiabatic, not vertical, IPs and EAs. PA8/06²² is a database of eight zero-point-exclusive proton affinities. Geometries for the PA8/06 database are obtained with the MP2(full)/6-311G(2df,p) method.^{28,29}

2.3. Alkyl Bond Dissociation Energy (ABDE12). The two databases for alkyl bond dissociation energies, ABDE4/05 and ABDEL8, were found to behave similarly in preliminary work, and we joined them in ABDE12. The ABDE4/05 database^{12,15,16} contains four bond dissociation energies of small R–X organic molecules, with R = methyl and isopropyl and X = CH₃ and OCH₃. ABDEL8⁶ contains a set of eight R–X bond dissociation energies including larger molecules, with R = ethyl and *tert*-butyl and X = H, CH₃, OCH₃, OH. For the 12 considered bonds, D_0 values are taken from a paper by Izgorodina et al.¹⁶ and converted to reference D_e values by using B3LYP/6-31G(d) zero-point vibrational energies scaled with a scale factor of 0.9806.

2.4. Hydrocarbons Difficult Cases (HC7/11). The HC7 database^{23,24} consists of seven difficult cases involving medium-range correlation energies in hydrocarbons. HC7 is the combination of the HC5 database with two isodesmic reactions (involving adamantane and bicyclo[2.2.2]octane) that were singled out as difficult cases by Grimme. All geometries were obtained with the MP2/6-311+G(d,p) method.^{28,29} The original reference data for this database have been published in a previous paper,²⁴ and some inconsistencies were recently corrected.⁶

2.5. Barrier Heights (HTBH38/08, NHTBH38/08). The HTBH38/08 database contains 38 transition state barrier heights for 19 hydrogen transfer (HT) reactions, 18 of which involve radicals as reactants and products.^{12,17,18} NHTBH38/08 consists of three databases containing 38 transition state barrier heights for non-hydrogen-transfer (NHT) reactions. The individual databases contain 12 barrier heights for heavy-atom transfer reactions, 16 barrier heights for nucleophilic substitution (NS) reactions, and 10 barrier heights for non-NS unimolecular and association reactions. Fourteen data points in this database were revised in 2008²⁵ and collected with other data in the DBH24/08 subset. Any of the data that were updated in DBH24/08 were updated in these databases, which are now renamed HTBH38/08 and NHTBH38/08. All geometries are obtained with the QCISD/MG3 method.^{7,26,27}

2.6. Noncovalent Interaction (NCCE31/05). Several databases have been developed in our group for various kinds of noncovalent interactions, in particular, HB6/04,²¹ CT7/04,²¹ DI6/04,²¹ WI7/05,¹³ and PPSS/05.¹³ HB6/04 is a hydrogen bond database that consists of the equilibrium binding energies of six hydrogen-bonded dimers. The CT7/04 database consists of binding energies of seven charge transfer complexes. The DI6/04 database contains the binding energies of six dipole interaction complexes. The WI7/05 database consists of the binding energies of seven weak interaction complexes, all of which are bound by dispersion-like interactions. The PPSS/05 database consists of binding energies of five π–π stacking complexes. We used them here grouped in the NCCE31/05 database.²⁴ The geometries for the benzene dimers in the NCCE31/05 database are taken from Sinnokrot and Sherrill,¹¹ while geometries for all other molecules in this database are optimized with the MC-QCISD/3 method.³⁰

2.7. Atomic Energies (AE17). AE17 is composed of 17 total atomic energies of the atoms from H to Cl.⁸

2.8. Metals (SRMBE12, MRMBE5). In a recent paper,⁶ we rearranged the databases^{19,20} related to metal bond energies by dividing them into single-reference metal bond energies and multireference metal bond energies. We keep this new division in this paper, and we use the SRMBE12 and MRMBE5 subsets as presented in ref 6.

2.9. Main Group Bond Lengths (MGBL19). MGBL19 is a database of 19 experimental bond lengths of 15 small main-group molecules,¹⁵ and the experimental bond lengths are taken from a previous compilation by Hamprecht et al.⁹

3. COMPUTATIONAL DETAILS

The MG3S basis set¹⁰ and the ultrafine (99,590) Lebedev grid are used throughout the paper for all calculations. Restricted calculations were performed for closed-shell species, while unrestricted calculations were employed for open-shell species. In systems like the oxygen atom, each orbital is an eigenfunction of the single-electron orbital angular momentum operators l^2 and l_z . However, singly occupied p orbitals have different radial functions and orbital energies than doubly occupied ones, and the atomic Slater determinants are not eigenfunctions of the many-electron orbital angular momentum operators L^2 and L_z . All calculations in section 4 are exchange-only (no correlation), but all those in section 5 include correlation.

4. THE DFT-SPLINE IMPLEMENTATION

4.1. Exchange. The key component in the DFT-spline implementation is the change of variables from s to u , given by eq 5, and the inverse transformation given by

$$s = \sqrt{\frac{u}{1-u}} \quad (7)$$

We replace the canonical enhancement factor of eq 6 with a natural cubic spline, f_x :

$$E_x^{\text{GGA}} = \int d^3r \rho \epsilon_x^{\text{LSDA}}(\rho) f_x(u) \quad (8)$$

Given that a sufficient number of knots are provided to allow the spline to accurately describe the original curve, this implementation is capable of replicating the results of any GGA functional that can be expressed as eq 6.

We define our spline as a piecewise cubic polynomial that interpolates a series of j points at equidistant knots, u_j . A total number of n_{spline} knots are taken, with separation $u = 1/(n_{\text{spline}} - 1)$ in the interval $u \in [0,1]$. The spline is defined as³¹

$$f_x = A_j f_j + B_j f_{j+1} + C_j f''_j + D_j f''_{j+1}, u_j \leq u \leq u_{j+1} \quad (9)$$

with

$$A_j = \frac{u_{j+1} - u}{n_{\text{spline}}} \quad (10)$$

$$B_j = 1 - A = \frac{u - u_j}{n_{\text{spline}}} \quad (11)$$

$$C_j = \frac{1}{6}(A_j^3 - A_j)(1/n_{\text{spline}})^2 \quad (12)$$

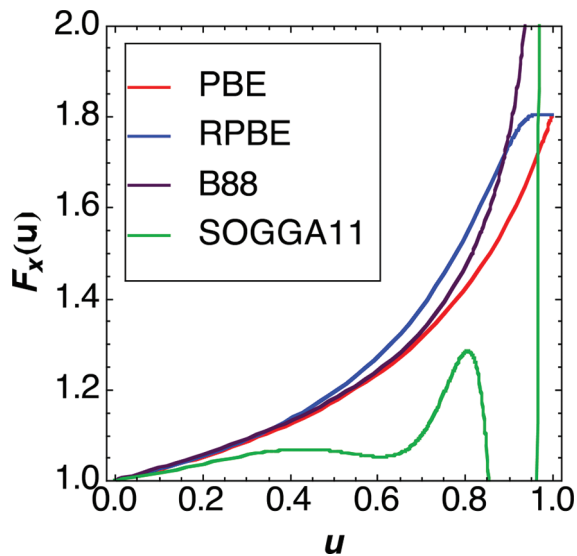


Figure 1. Enhancement factors for different exchange functionals in the new variable u .

$$D_j = \frac{1}{6}(B_j^3 - B_j)(1/n_{\text{spline}})^2 \quad (13)$$

$$u_j = (j-1)/(n_{\text{spline}} - 1) \quad (14)$$

and natural conditions on second derivatives at the end points

$$f''_1 = f''_{n_{\text{spline}}} = 0 \quad (15)$$

The coefficients of the spline are calculated once, by means of a tridiagonal matrix algorithm based on Gaussian elimination³¹ and then stored. The value of the spline and its first derivative are then calculated on the fly from the stored coefficients at each point of the DFT integration grid. This results in an efficient algorithm, which is not more expensive than evaluating conventional exchange functionals. The evaluation of the enhancement factor in a standard DFT implementation is a negligible part of the cost in a DFT calculation, and the spline implementation retains this advantage.

4.2. Implementation of Common GGA Functionals by Means of the DFT-Spline Algorithm. In this work, we implemented some of the most successful GGA exchange functionals by using the DFT-spline algorithm in a modified version of the Gaussian 09 program.³² The functionals considered are PBE,³ RPBE,⁴ B88,⁵ and SOGGA11.⁶

The four enhancement factors are shown in Figure 1, and their formulations are obtained from the original definitions of $F(s)$ by applying the transformation in eq 7. The enhancement factors in the transformed variable were used to calculate the ordinates at equidistant knots of the abscissa u . The DFT-spline algorithm was used to interpolate the points, and we expect its performances to be directly influenced by the number of the knots used by the algorithm.

As pointed out in the original paper, SOGGA11 has an oscillating behavior for large u . Although the spline implementation allows an easy fix for such a problem, this is not the purpose of the present work.

We studied the convergence of the results obtained with the DFT-spline implementation as a function of the total number of

Table 1. Root Mean Square Deviation (RMSD/E_h)^a from the Absolute Atomic Energies Obtained with the Usual Implementation as a Function of the Number of the Knots in the Spline (*n*_{spline}) for Four Exchange Functionals

<i>n</i> _{spline}	PBE (XO) ^b	RPBE (XO) ^b	B88 (XO) ^b	SOGGA11 (XO) ^b
11	1×10^{-5}	2×10^{-4}	1×10^{-3}	2×10^{-2}
21	9×10^{-7}	8×10^{-6}	5×10^{-4}	6×10^{-3}
101	2×10^{-9}	8×10^{-9}	5×10^{-6}	5×10^{-6}
201	3×10^{-10}	4×10^{-10}	2×10^{-7}	6×10^{-8}
1001	$\leq 1 \times 10^{-10}$	$\leq 1 \times 10^{-10}$	1×10^{-8}	2×10^{-9}
2001	$\leq 1 \times 10^{-10}$			

^a 1 E_h = 1 hartree = 27.2114 eV. ^b XO denotes that these are exchange-only calculations (no correlation)

knots, *n*_{spline}, for these four exchange functionals by comparing them to those obtained from the usual implementation of the same functionals. For this study, we used exchange-only density functionals to calculate SCF atomic energies of the first 17 atoms (H to Cl), performing unrestricted calculations with the MG3S²² basis set. The root-mean-square deviations (RMSDs) in hartrees from the energies obtained with the usual implementation are presented as a function of *n*_{spline} in Table 1.

The results in Table 1 show that the spline implementation is capable of replicating conventional results for all considered functionals. In general, there is good agreement between the atomic energies obtained with the DFT-spline implementation and the usual implementation. For PBE and RPBE, RMSDs smaller than 2×10^{-4} are obtained with the surprisingly small value of *n*_{spline} = 11. For more complicated functionals, like B88 and the SOGGA11 exchange, a slightly larger number of points is necessary to reach similar convergence. At the extreme value of *n*_{spline} = 2001, the atomic energies calculated with the DFT-spline and the canonical implementation are identical within 10^{-10} E_h. However, we find that *n*_{spline} = 101 (corresponding to one point every 0.01 *u* units) provides a RMSD smaller than 5×10^{-5} E_h for all functionals, and this value is sufficient for the description of atomic energies to chemical accuracy.

In order to confirm these results on molecular energies, we used the large database described in section 2. For each of the 350 atomic and molecular energy calculations required to compute the energetic part of the database, we calculated the difference between the absolute energies obtained with the DFT-spline implementation and those obtained from the usual implementation without fitting. These calculations are performed by combining the DFT-spline implementation of the exchange with *n*_{spline} = 101 with correlation functionals calculated using the usual implementation. The B88 exchange functional was coupled with the LYP correlation to obtain BLYP energies. PBE and RPBE were coupled with PBE correlation, and SOGGA11 exchange was coupled with SOGGA11 correlation. The RMSDs are presented in Table 2, and they confirm the excellent performance of the DFT-spline implementation in the calculations of the considered functionals. In particular, all of the results on the larger molecular database are very similar to those obtained for the smaller atomic set using the same number of points, *n*_{spline} = 101.

As a further validation of the performance of the new implementation, we used the DFT-spline results to calculate the mean unsigned errors of the 303 energetic chemical data in the considered databases. Results for the MUE of these data do

Table 2. Root Mean Square Deviation (RMSD/E_h) of Results Obtained Using *n*_{spline} = 101 from the Absolute Energies Obtained Without Fitting for the 350 Atomic and Molecular Single-Point Energies in the Database^a

functional	RMSD
PBE	5×10^{-9}
RPBE	1×10^{-8}
BLYP	5×10^{-6}
SOGGA11	7×10^{-6}

^a These calculations include both exchange and correlation, but the spline is applied only to exchange in this table.

not differ from those obtained with the nonfitted implementation up to a level of precision of 10^{-3} kcal/mol.

5. SENSITIVITY STUDY

The dependence of the exchange-correlation functional on *s* or *u* plays a crucial role in the development of density functionals since it entirely determines the performance of a GGA functional. Values at some knots are fixed by physical constraints, e.g., the uniform electron gas fixes the value of the gradient enhancement factor to be 1 at *u* = 0. The known second order coefficient for the density gradient expansion fixes the value of the first derivative with respect to *u* at *u* = 0, but the global *u* dependence is unknown. It is generally believed that the significant region for the description of chemical properties lies between $0 \leq s \leq 3$,^{33,34} corresponding to *u* in the range 0–0.9, but more detailed information about which *s* or *u* region contributes most to each property is hard to obtain. An advantage of the DFT-spline implementation lies in the fact that it provides a simple tool to investigate the shape of the enhancement factor as a function of the reduced density gradient variable.

A natural cubic spline implementation for correlation is not as straightforward as the one for exchange because the correlation enhancement factors generally depend on a spin variable ζ as well as the density and density gradient (see the Appendix). In order to perform the sensitivity study, we modify the exchange or correlation component of the GGA functionals under study by multiplying by a spline factor, in particular

$$E_x^{\text{GGA}} = \int d^3 r \varepsilon_x^{\text{GGA}}(\rho, s) f_x(u) \quad (16)$$

for exchange and

$$E_c^{\text{GGA}} = \int d^3 r \varepsilon_c^{\text{GGA}}(\rho, s, \zeta) f_c(u) \quad (17)$$

for correlation, where *f*_x and *f*_c are both natural cubic splines of the form of eq 9. The base spline is a trivial one obtained by setting the value to *f* = 1 for both the exchange and the correlation at all 21 knots. The sensitivity analysis to different ranges is performed by modifying the base spline by either increasing or decreasing the value of *f* at one single knot, *j* + 1, by 5%, in order to obtain a perturbation at the corresponding value of *u*.

Examples of the resulting splines are shown in Figure 2, where the first and ninth points are brought from 1.0 to 1.05 to obtain *f*₊ and from 1.0 to 0.95 to obtain *f*₋. The 5% value was chosen because it is large enough for the perturbation to be significant but is still small enough to avoid extensive ringing near the perturbed point (as can be seen in Figure 2). For each modification

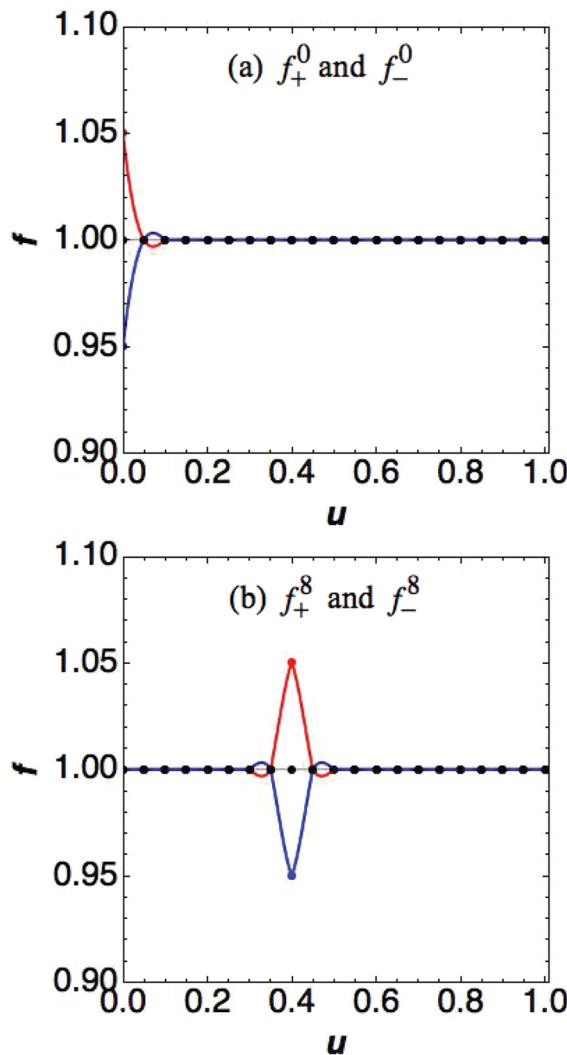


Figure 2. Perturbation of the base spline (black) to form (a) f_+^0 (red) and f_-^0 (blue) and (b) f_+^8 (red) and f_-^8 (blue).

of each exchange or correlation functional, we performed full SCF calculations on the chosen database.

For every modification of the base spline, we calculate the sensitivity (S) of the results by using the following formula:

$$S = \frac{\Delta^+ + \Delta^-}{2} \quad (18)$$

with

$$\Delta^\pm = \pm \frac{1}{\delta} \frac{\text{MUE}(\pm \delta) - \text{MUE}(0)}{\text{MUE}(0)} \quad (19)$$

where δ is the relative perturbation applied (± 0.05 in our case). Then Δ^\pm measures the sensitivity of the properties as a function of the perturbation applied, for example, if a positive perturbation of 5% in u decreases the MUE by 10%, we have $\Delta^+ = -0.10/0.05 = -2$. At the same time, if a negative perturbation in u worsens the results by 5%, we have $\Delta^- = 0.05/-0.05 = -1$. The sensitivity in this case will be $S = (-2 - 1)/2 = -1.5$.

Results for the sensitivity study of the four considered exchange functionals and two correlation functionals are discussed in the next sections. PBE and SOGGA11 were chosen for

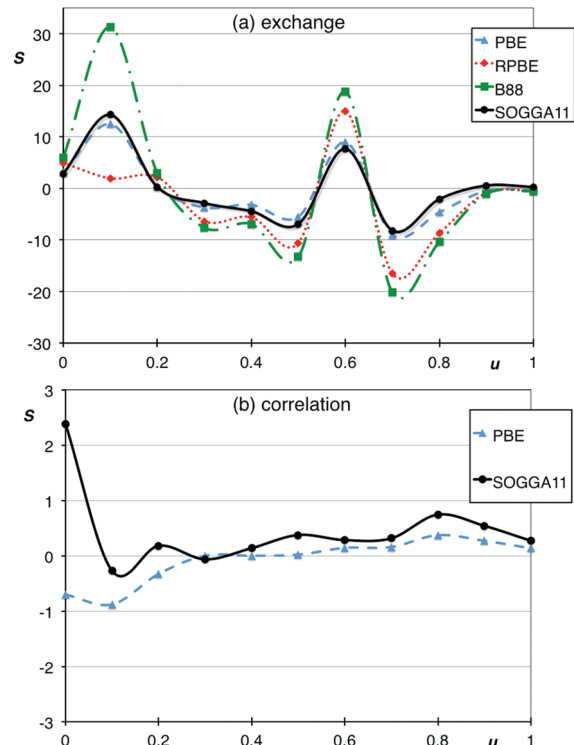


Figure 3. Sensitivity study to variation of (a) f_x and (b) f_c as a function of u for MGAE109/05.

study as representative correlation functionals. All four exchange functionals and both correlation functionals studied here satisfy the uniform electron gas constraint at $u = 0$.

The correlation energy is on average an order of magnitude smaller than the exchange energy, and effects of a given percentage change in the correlation functional therefore tend to be much smaller than those for changing the exchange functional. For these reasons, all plots for correlation are reported with a smaller scale.

5.1. Main Group Atomization Energies (MGAE109/05). The effects of the perturbations at localized regions of u on the main-group atomization database are collected in the parts a and b of Figure 3. All four of the exchange functionals are sensitive to changes over almost all of the values of u . We can distinguish two regions of importance, one around $u = 0.1$ and another between $u = 0.5$ and $u = 0.8$. It is interesting to note a significant sensitivity at $u = 0.8$ ($s = 2$) and even higher, which corresponds to a region that was previously thought to have less significant importance.

For the correlation functional, the results are mainly sensitive in the small u region, including the UEG point at $u = 0$. For correlation too, we find an unexpected sensitivity at large values of u , around $u = 0.8$.

In order to make these results more concrete and less abstract, let us consider an example. Consider the PBE functional; the MUE per bond for PBE with this database is 2.99 kcal/mol. Decreasing the enhancement factor by 5% at $u = 0.1$ changes this to 1.69 kcal/mol (a 44% decrease), whereas increasing it by 5% at $u = 0.1$ changes the MUE to 5.41 kcal/mol (an 81% increase). Therefore, S is the average of 16.2 and 8.7, which yields the plotted value of 12.5. In general, a positive S means that the accuracy is increased by decreasing the density functional at that point.

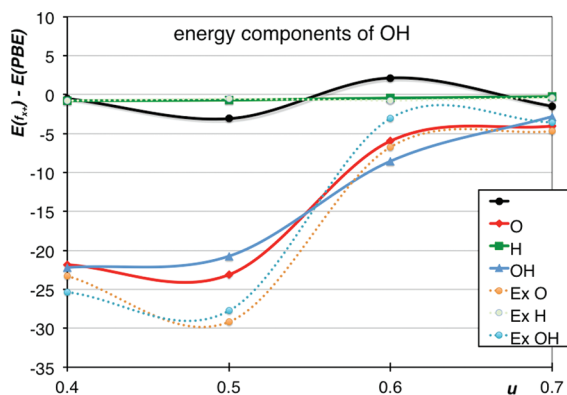


Figure 4. Analysis of the changes in the energy components of the OH radical and its bond dissociation products upon increasing f_x from 1.0 to 1.05 at selected values of u . The curves labeled Ex show changes in exchange energy of O, H, and OH. The curves labeled O, H, and OH show changes in the total energy of the atoms and molecule. The black curve is the change in bond energy (total energy of the atoms minus total energy of the molecule).

To illustrate the origin of the different behavior as a function of u , we pick the OH radical as a representative molecule from the MGAE109/05 database. The PBE functional has an error of 2.4 (to make it easier to read, all energies in the rest of this discussion are expressed in kcal/mol and rounded to the nearest tenth) for the OH bond energy (accurate, 107.1; unaltered PBE, 109.5), which is similar to the mean unsigned error of 3.0, and its behavior around $u = 0.6$ is also similar to the average over the whole database.

For the OH molecule, the oxygen atom, and the hydrogen atom, we plot in Figure 4 the differences between the absolute energies (solid) and the exchange energies (dotted) obtained using the base spline and that obtained using the perturbed spline f_{x+} , with 5% positive perturbations in the range $0.4 \leq u \leq 0.7$. The plot also shows the change in the bond energy.

The differences for the hydrogen atom are not significant for both the exchange (changes from -0.4 to -0.8 kcal/mol) and the total energies (changes from -0.3 to -0.8), and it is clear that the changing in behavior of the atomization energy curve is given mainly by the different sensitivity of the OH molecule and the O atom. Furthermore, although the correlation energy does change (because the SCF calculation with a perturbed exchange functional leads to a perturbed density), in all cases (atoms and molecules) the change is small (usually of magnitude less than 0.1, always of magnitude less than 0.2). This shows that the change in the direct energy contribution of the density functional is mainly due to the change in exchange energy of O and OH.

The exchange energy of O before the perturbation is -5112.7 , while that of OH is -5347.7 . The contribution of exchange to the bond energy (exchange energy of O plus H minus that of OH) is 44.9 kcal/mol.

Since the perturbation is positive, the exchange energy increases in magnitude, becoming more negative. For a perturbation at $u = 0.6$, the exchange energy of O becomes -5119.5 , a change of -6.7 , while that of OH becomes -5350.7 , a change of only -3.1 . The contribution of exchange to the bond energy becomes 40.5 kcal/mol, a perturbation of the exchange contribution to the bond energy of -4.4 . However, the perturbation changes the orbitals. While the total energy of O changes

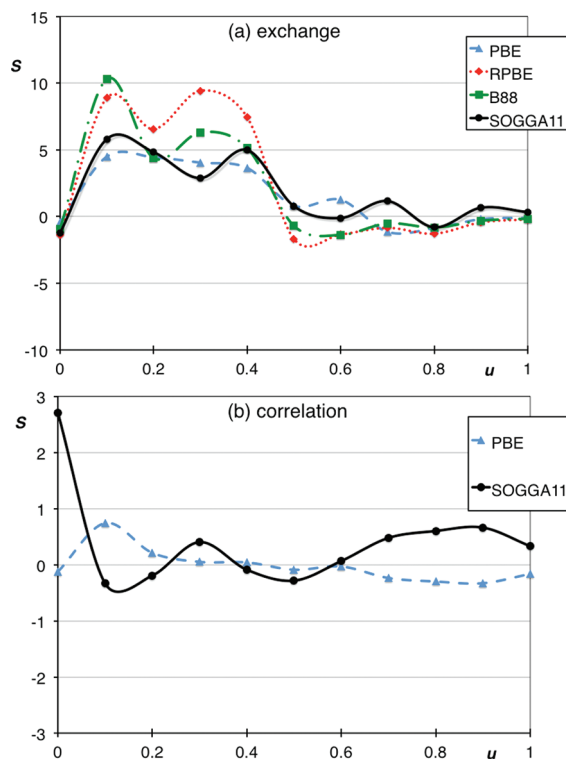


Figure 5. Sensitivity study to variation of (a) f_x and (b) f_c as a function of u for IP13/03.

by -6.0 , that of OH is more sensitive, and it changes by -8.6 . The net change to the bond energy is $+2.2$, raising the error from 2.2 to 4.6. A negative perturbation produces changes of a similar magnitude but in the opposite direction. The large magnitude of the individual terms illustrates the well-known fact that quantum mechanics involves large cancellations of absolute energy contributions to produce chemical results like bond energies, and the competing effects of this example make it more understandable that the sign of S can change as a function of u . For example, as seen in the figure, the exchange curves of O and OH cross so that a positive perturbation at $u = 0.4$ changes the exchange energy of O by -23.3 and that of OH by -25.3 . Hence, the exchange contribution to the bond energy is perturbed in the opposite direction of that at $u = 0.6$, and the bond energy change is also in the opposite direction. The purpose of the sensitivity analysis is not to trace all of these details through the SCF calculations and the changes in orbitals but rather to see if changes in the exchange and correlation functional in certain regions of u have systematic effects on the accuracy of prototype chemical properties, so that one knows which regions of u space are important for more systematic improvement of exchange–correlation functionals for better chemical predictions in the future.

5.2. Ionization Potentials (IP13/03). Results for the IP13/03 database are collected in Figure 5. Ionization potentials are sensitive to the small u region of the exchange functional, $0.1 \leq u \leq 0.4$. The errors are most sensitive to changes in the correlation functional at $u = 0$ and at $u \geq 0.7$.

5.3. Electron Affinities (EA13/03). Results for the EA13/03 database are collected in Figure 6. The effects of changes in the exchange functional on electron affinities are similar to those for ionization

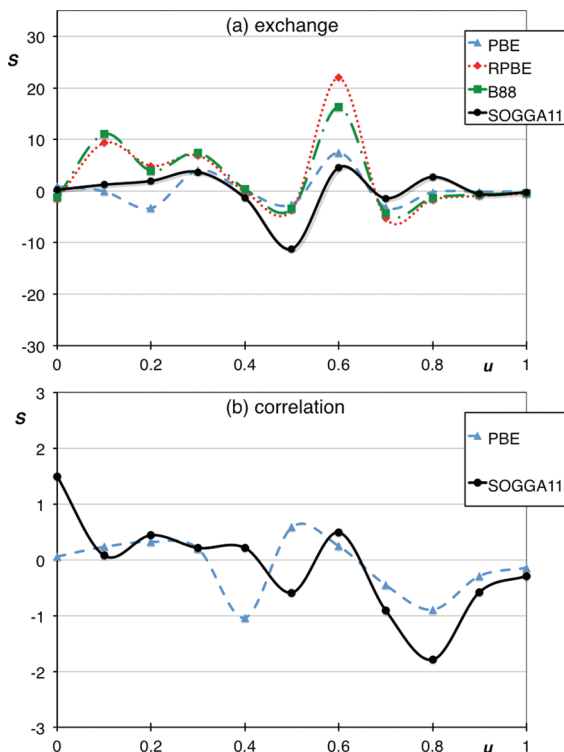


Figure 6. Effects of the variation of (a) f_x and (b) f_c as a function of u on the MUE of EA13/03.

potentials, with a broad sensitive region between $0.1 \leq u \leq 0.3$. A key difference in these two properties is the region around $u = 0.7$, which is more important for the electron affinities than for the ionization potentials.

For the correlation, we notice sensitive effects in regions where the exchange is less affected, in particular $u = 0.8$.

Comparing Figures 3–6, an interesting conclusion emerges. In particular, all four exchange functionals could all be improved for all three properties by decreasing the exchange enhancement factor around $u = 0.6$. However, decreasing the SOGGA correlation function at $u = 0.8$ improves the atomization energies and IPs but makes the EAs worse. The latter shows the limitations of GGAs; they are not flexible enough to fit all properties, but the former shows the inflexibility of prechosen functional forms, not of GGAs per se.

5.4. Proton Affinities (PA8/06). Results for proton affinities are presented in Figure 7. This property has less sensitivity than ionization potentials and electron affinities, with the most significant centered at about $u = 0.1$ for both the exchange and the correlation.

5.5. Alkyl Bond Dissociation Energies (ABDE12). Results for alkyl bond dissociation energies are reported in Figure 8.

Results for the exchange are affected in two main regions, one at $u = 0.1$ and the other one at $u = 0.5–0.7$. It is interesting to note that all functionals seem improvable at $u = 0.1$, but if the goal is to obtain a good overall functional (as it was for SOGGA11), performances in that region for ABDE12 must be balanced with those for MGAE109/05, which is also very sensitive here but in the opposite direction. This shows why it is important to have both atomization energies and bond energies in training and test sets.

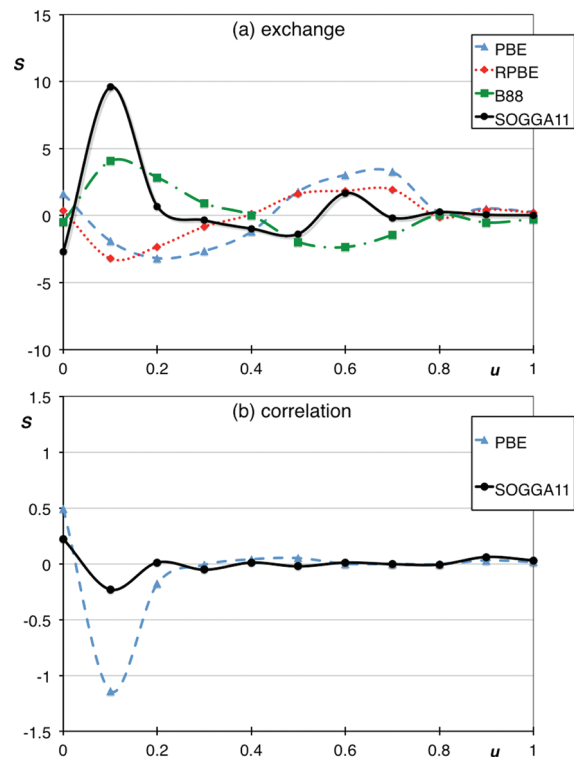


Figure 7. Effects of the variation of (a) f_x and (b) f_c as a function of u on the MUE of PA8/06.

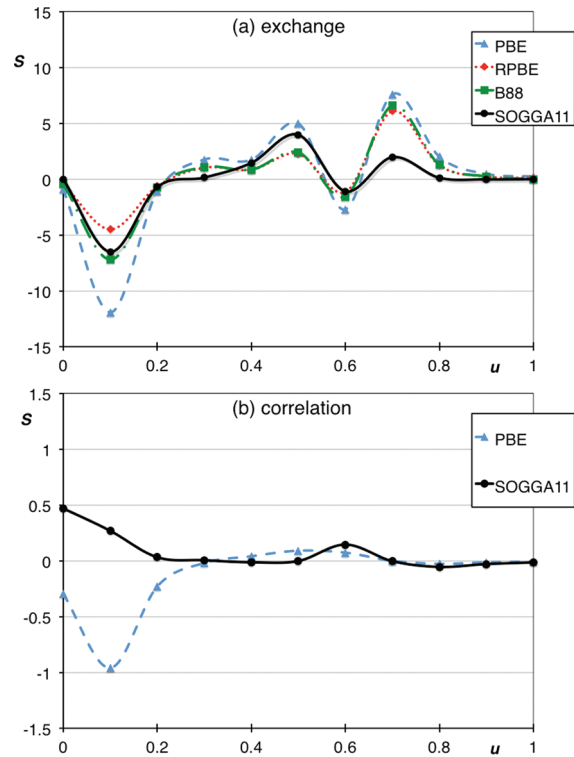


Figure 8. Effects of the variation of (a) f_x and (b) f_c as a function of u on the MUE of ABDEL12.

Correlation effects are once again smaller than those for exchange, with a sensitive region for alkyl bond energies at $u = 0.1$.

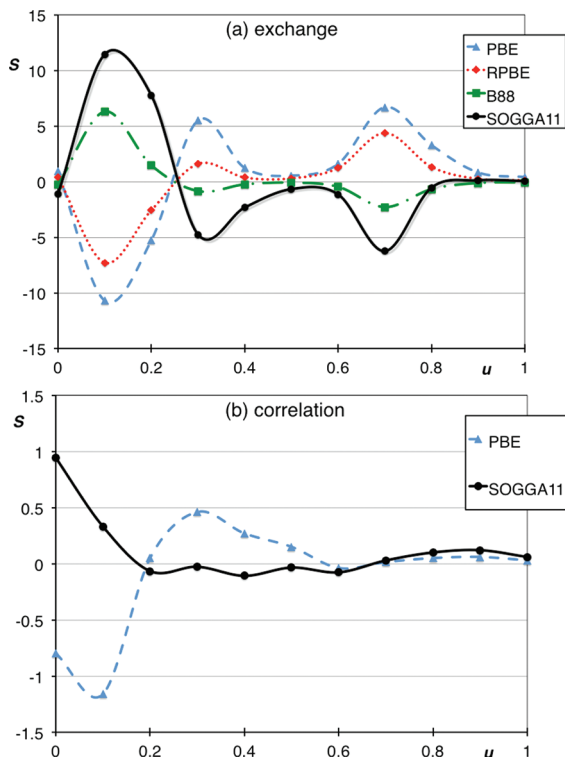


Figure 9. Effects of the variation of (a) f_x and (b) f_c as a function of u on the MUE of HC7.

5.6. Difficult Hydrocarbon Cases (HC7/11). Results for the difficult hydrocarbon cases are presented in Figure 9.

The most sensitive regions for the exchange are again the regions around $u = 0.1$ and around $u = 0.7$. This implies that improving GGA functionals for this property must be carefully balanced with the performances for atomization energies and alkyl bond dissociation energies.

The sensitivity to changes in the correlation functional is very small for $u \leq 0.6$ and almost zero at larger values of u .

5.7. Barrier Heights (HTBH38/08, NHTBH38/08). Results for the HTBH38/08 database are collected in Figure 10, and results for NHTBH38/08 are presented in Figure 11. Barrier heights have long been a difficult problem for DFT, and these figures help us to understand why.

Consider first the more important exchange functional. Two of the exchange functionals have positive sensitivity at $u = 0.1$ for both kinds of barriers, but the other two show opposite sensitivity. For the two functionals with opposite signs of S , improving the performance for one kind of barrier will worsen it for the other. Furthermore, for all four functionals, the sensitivity fluctuates wildly (as a function of u) for NHTBH38/08. Restricted analytic forms may not have the flexibility to be optimum for all regions of u .

Barrier heights are much less sensitive to the correlation functional, confirming what we expected from previous experience. The present results are more definitive though, since they do not suffer from the possible inadequacy of choosing an insufficiently flexible functional form.

5.8. Noncovalent Interactions (NCCE31/05). Sensitivity results for noncovalent interactions are presented in Figure 12. The sensitivity of this property to the exchange functional is spread out over a wide range of u . Interestingly, the

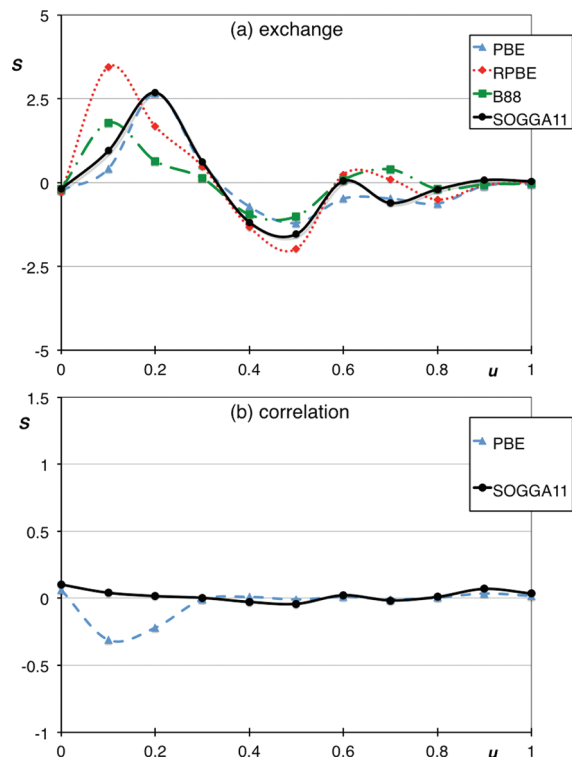


Figure 10. Effects of the variation of (a) f_x and (b) f_c as a function of u on the MUE of HTBH38/08.

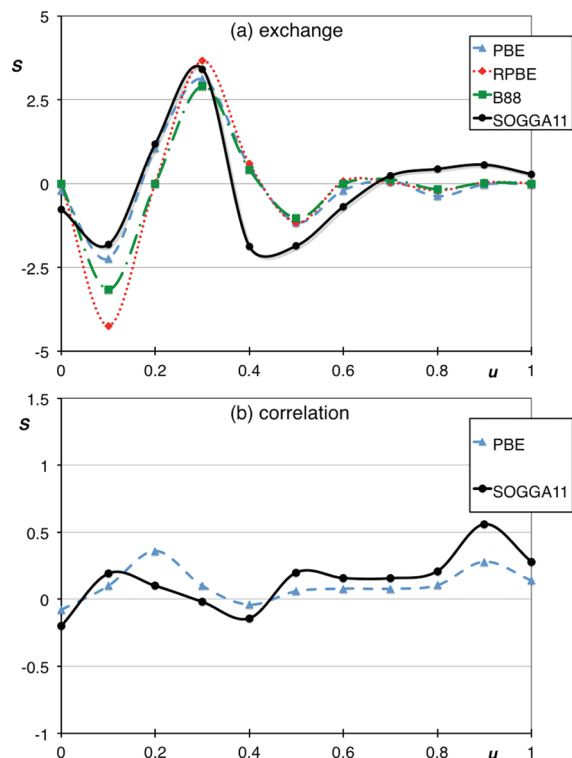


Figure 11. Effects of the variation of (a) f_x and (b) f_c as a function of u on the MUE of NHTBH38/08.

sensitivity to the exchange functional is smallest for SOGGA11, perhaps indicating that this functional is close to optimal

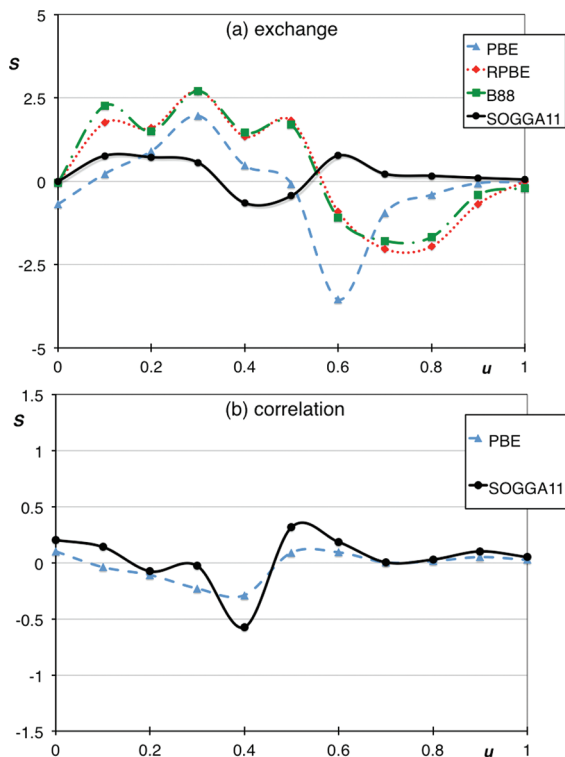


Figure 12. Effects of the variation of (a) f_x and (b) f_c as functions of u on the MUE of NCCE31/05.

(the first derivative with respect to changes vanishes for an optimum function).

From a more general perspective, it is known that the behavior of the enhancement factor at large values of the reduced density gradient s affects the performance of the exchange functional for noncovalent interactions.^{35–38} For example, functionals (such as B88) with enhancement factors that approach large values or infinity at large s have a very different performance for noncovalent interactions than functionals (such as PBE) with enhancement factors that asymptotically reach a small value. This fact is clearly reflected in the mean signed errors of each group of functionals for the noncovalent interaction data set. For example, B88 underestimates the attractive noncovalent interactions by about 3 kcal/mol, while PBE overestimates them by about 1 kcal/mol. Our sensitivity analysis, however, tests the performance of each functional for small perturbations of the enhancement factor, and our plots, like all sensitivity analyses based on small perturbations, are incapable of showing this behavior. This is one of the disadvantages of sensitivity analysis in general.

In a recent paper, Johnson et al.,³⁸ by analysis of the electron density, found by another route that noncovalent interactions are indeed sensitive to a large range of s . Their analysis included larger molecules of biological interest, with similar conclusions to those drawn from our sensitivity analysis, which, however, adds the important observation that most of the sensitivity is coming from the exchange functional. Correlation contributes to the sensitivity in the region around $u = 0.4$ –0.5, corresponding to $s = 0.8$ –1, but the effect is smaller than for exchange.

One encouraging result is that for the exchange functional at $u = 0.3$. Figures 3–11 show that the sensitivities of the PBE, RPBE, and B88 functionals are all positive or small at this u value

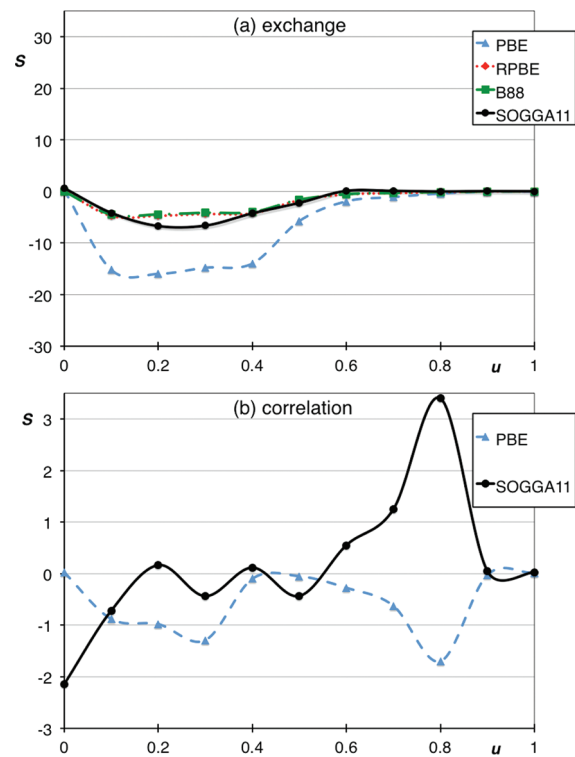


Figure 13. Effects of the variation of (a) f_x and (b) f_c as functions of u on the MUE of AE17.

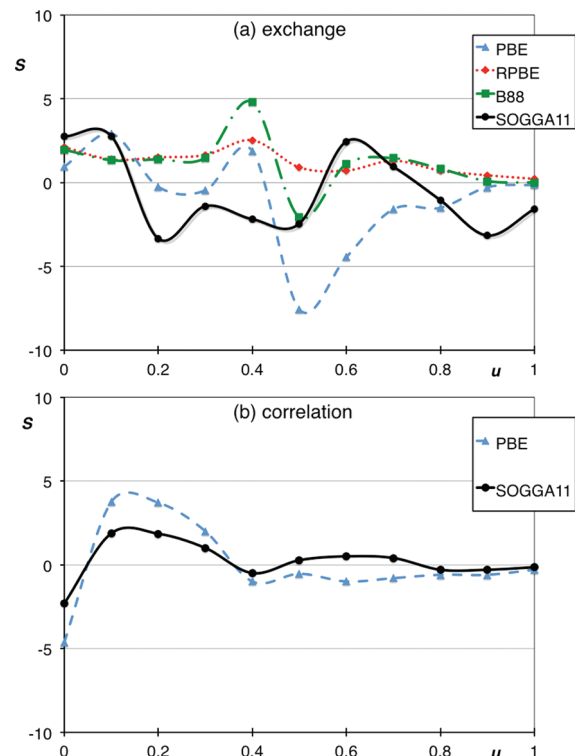


Figure 14. Effects of the variation of (a) f_x and (b) f_c as a function of u on the MUE of SRMBE12.

for the wide range of nonmetallic molecular properties represented in these nine figures. Thus, decreasing the exchange at this

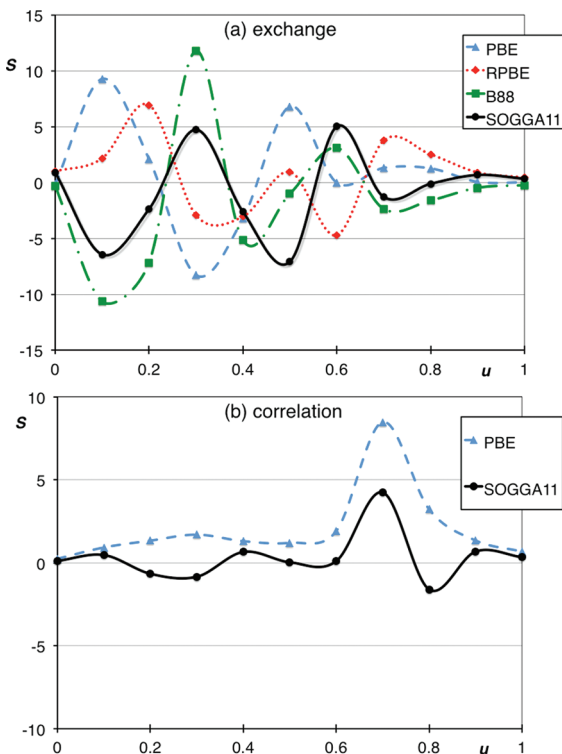


Figure 15. Effects of the variation of (a) f_x and (b) f_c as a function of u on the MUE of MRMBE5.

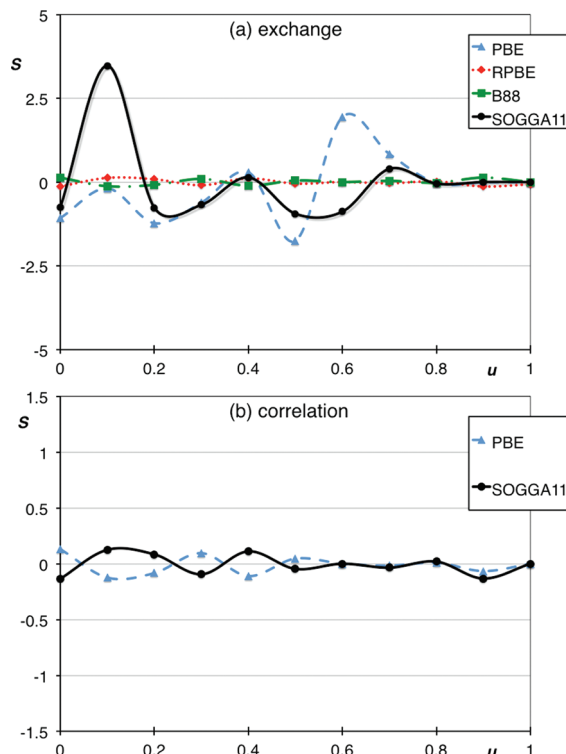


Figure 16. Effects of the variation of (a) f_x and (b) f_c as a function of u on the MUE of MGBL19.

u value should improve those functionals broadly. If we had not already optimized the exchange and found that these functionals have too much exchange at this u value (see Figure 1), this might have led us to discover this. However, for SOGGA11, S is negative in Figure 9, indicating that some values would improve and some would get worse if it were decreased further.

5.9. Atomic Energies (AE17). Results for the 17 total atomic energies of the atoms from H to Cl are collected in Figure 13. Atomic energies show a broad sensitive region for the PBE functional in the region $0.1 \leq u \leq 0.5$; this is an indication of systematic error in that the functional could be improved by increasing the exchange. However, as is clear from the discussion in the previous subsection, increasing the exchange functional in that region would make many molecular properties worse, at the expense of improving atomic absolute energies.

At $u = 0$ and at $u = 0.8$, there is basically no sensitivity for all exchange functionals, while the correlation functional is most sensitive in these regions.

5.10. Metals (SRMBE12, MRMBE5). The results for single-reference metal bond energies (SRMBE12) and the multi-reference metal bond energies (MRMBE5) are reported in Figures 14 and 15.

Compounds containing transition metals are difficult to treat with DFT, and the results for the exchange confirm this prediction. It is hard to find common ground from the sensitivity study, but in general we can say that SRMBE12 is less sensitive to changes in the exchange functional than is MRMBE5, whereas the opposite is true for correlation. SRMBE12 shows sensitivity in the entire range of u . Both correlation functionals show sensitivity in the small u region for SRMBE12 and a pronounced sensitivity around $u = 0.7$ for MRMBE5.

The different behavior of the SOGGA11 sensitivity in Figure 14 as compared to the other three can be understood to some extent by the behaviors shown in Figure 1, except at $u = 0.6$. However, Figure 15 is very hard to understand.

5.11. Main Group Bond Lengths (MGBL19). Results on the geometries database MGBL19 are reported in Figure 16. The sensitivity of the bond length to changes in the exchange are quite small, with two interesting regions at $u = 0.1$ and $u = 0.6$. The effects of the correlation are also very small.

6. CONCLUDING REMARKS

We presented in this article an implementation of four common GGA exchange functionals by means of a natural cubic spline. We showed that the spline is able to reproduce the unfitted results very accurately. This opens the door to future work in which density functionals can be defined directly in terms of splines, without being constrained by guessed functional forms. Other advantages of the DFT-spline implementation include very convenient calculation of the first and second derivatives, offering a simpler implementation in quantum chemistry codes for any GGA functional, and the possibility to create new fitted functionals that are not subject to Runge's phenomenon of oscillation for high-order interpolating polynomial functions.

By using multiplicative factors defined in terms of spline functions, we were able to study the exchange and correlation components of GGAs to various regions of the reduced density for 12 energetic chemical databases and one bond-length database. This task was hardly possible before, with the usual DFT implementation. In general, if we consider the results for the

exchange, we usually find reasonably good agreement for all considered functionals as to which are the sensitive regions of u . The two correlation functionals are, however, usually sensitive to other regions.

In some cases, the sensitivity analysis shows the limitations of GGAs in that changes of the density functionals in a given direction make one property better and another worse. This is particularly clear for the exchange functional in the range $0 \leq u \leq 0.5$. For example, when a negative perturbation is applied in that range, properties such as MGAE109/05, HC7, PA8/06, NCCE31/05, and MGBL19 often improve, presenting a positive sensitivity, but properties such as ABDEL12 and AE17 often worsen, with negative sensitivity. Barrier heights are less sensitive than other properties, but hydrogen transfers (HTBH38/08) and non-hydrogen transfers (NHTBH38/08) present different sensitivities to changing the exchange in the same region. At large values of u , sensitivity is always reduced compared to the small u region, but some databases such as IP13/03, PA8/06 HTBH38/08, NHTBH38/08, and AE17 present basically no sensitivity to variations in the exchange at large u , while the others present some sensitivity, with contrasting behaviors.

Perturbation of the correlation functional always produces smaller effects, but also in this case we can find examples of different behaviors in the $0 \leq u \leq 0.5$ range, for example, positive values of S for properties such as MGAE109/05, IP13/03, and SRMBE12 and negative values for EA13/03 and PA8/06. Thus, any attempt at optimization involves a trade-off where some quantities get better and others get worse. We find that some databases, e.g., MGAE109/05, PA8/06, ABDEL12, HC7, HTBH38/08, NCCE31/05, SRMBE12, and MGBL19, do not have significant sensitivity at large values of u , while others have small but non-negligible sensitivity. In particular, it is interesting to note the different behavior of the two barrier height databases (NHTBH38/08 and HTBH38/08) and the large sensitivity of AE17 in this large u region, as opposed to what was found for exchange.

■ APPENDIX: FORMULAS FOR THE SPIN-UNRESTRICTED CASE

Exchange. The exchange energy for a spin-polarized system ($\rho^\uparrow \neq \rho^\downarrow$) is evaluated in the usual way from the exchange functional for a spin-unpolarized system ($\rho^\uparrow = \rho^\downarrow$) by using the spin-scaling relation:

$$E_x\{\rho^\uparrow, \rho^\downarrow\} = E_x[2\rho^\uparrow]/2 + E_x[2\rho^\downarrow]/2 \quad (\text{A.1})$$

where $E_x[\rho] \equiv E_x\{\rho/2, \rho/2\}$ is calculated with eq 1 from the main text.

Correlation. The spin-polarized case for correlation is more complicated, and various approaches are used in the literature. The PBE and SOGGA11 correlation functionals (which are the only ones considered here) use an enhancement factor that depends upon the relative spin polarization $\xi = (\rho^\uparrow - \rho^\downarrow)/\rho$:

$$E_c\{\rho^\uparrow, \rho^\downarrow\} = \int d^3r \rho\{\varepsilon_c^{\text{LSDA}}(\rho, \xi) + H(\rho, u, \xi)\} \quad (\text{A.2})$$

■ AUTHOR INFORMATION

Corresponding Author

*E-mail: truhlar@umn.edu.

■ ACKNOWLEDGMENT

This work was supported in part by the National Science Foundation under grant no. CHE09-56776.

■ REFERENCES

- (1) Kohn, W.; Becke, A.; Parr, R. *J. Phys. Chem.* **1996**, *100*, 12974.
- (2) Becke, A. *D. J. Chem. Phys.* **1996**, *107*, 8554–8560.
- (3) Perdew, J. P.; Burke, K.; Ernzerhof, M. *Phys. Rev. Lett.* **1995**, *77*, 3865–3868.
- (4) Hammer, B.; Hansen, L.; Norskov, J. *Phys. Rev. B* **1999**, *59*, 7413–7421.
- (5) Becke, A. D. *Phys. Rev. A* **1987**, *38*, 3098–3100.
- (6) Peverati, R.; Zhao, Y.; Truhlar, D. G. *J. Phys. Chem. Lett.* **2011**, *1991*–1997.
- (7) Pople, J.; Head-Gordon, M.; Raghavachari, K. *J. Chem. Phys.* **1987**, *87*, 5968–5975.
- (8) Chakravorty, S.; Gwaltney, S.; Davidson, E.; Parpia, F.; Fischer, C. *Phys. Rev. A* **1993**, *47*, 3649–3670.
- (9) Hamprecht, F.; Cohen, A.; Tozer, D. J.; Handy, N. C. *J. Chem. Phys.* **1997**, *109*, 6264–6271.
- (10) Lynch, B. J.; Zhao, Y.; Truhlar, D. G. *J. Phys. Chem. A* **2003**, *107*, 1384–1388.
- (11) Sinnokrot, M. O.; Sherrill, C. D. *J. Phys. Chem. A* **2003**, *108*, 10200–10207.
- (12) Zhao, Y.; Schultz, N. E.; Truhlar, D. G. *J. Chem. Theory Comput.* **2005**, *2*, 364–382.
- (13) Zhao, Y.; Truhlar, D. G. *J. Phys. Chem. A* **2005**, *109*, 5656–5667.
- (14) Zhao, Y.; Schultz, N. E.; Truhlar, D. G. *J. Chem. Phys.* **2005**, *123*, 161103.
- (15) Zhao, Y.; Truhlar, D. G. *J. Chem. Phys.* **2005**, *125*, 194101.
- (16) Izgorodina, E.; Coote, M.; Radom, L. *J. Phys. Chem. A* **2005**, *109*, 7558–7566.
- (17) Zhao, Y.; Lynch, B. J.; Truhlar, D. G. *Phys. Chem. Chem. Phys.* **2005**, *7*, 43–52.
- (18) Zhao, Y.; González-García, N.; Truhlar, D. G. *J. Phys. Chem. A* **2005**, *109*, 2012–2018.
- (19) Schultz, N. E.; Zhao, Y.; Truhlar, D. G. *J. Phys. Chem. A* **2005**, *109*, 4388–4403.
- (20) Schultz, N. E.; Zhao, Y.; Truhlar, D. G. *J. Phys. Chem. A* **2005**, *109*, 11127–11143.
- (21) Zhao, Y.; Truhlar, D. G. *J. Chem. Theory Comput.* **2005**, *1*, 415–432.
- (22) Zhao, Y.; Truhlar, D. G. *J. Phys. Chem. A* **2006**, *110*, 10478–10486.
- (23) Zhao, Y.; Truhlar, D. G. *Org. Lett.* **2006**, *8*, 5753–5755.
- (24) Zhao, Y.; Truhlar, D. G. *Theor. Chem. Acc.* **2008**, *120*, 215–241.
- (25) Zheng, J.; Zhao, Y.; Truhlar, D. G. *J. Chem. Theory Comput.* **2009**, *5*, 808–821.
- (26) Curtiss, L.; Raghavachari, K.; Redfern, P.; Rassolov, V.; Pople, J. *J. Chem. Phys.* **1997**, *109*, 7764–7776.
- (27) Fast, P.; Sanchez, M.; Truhlar, D. *Chem. Phys. Lett.* **1999**, *306*, 407–410.
- (28) Moller, C.; Plesset, M. *Phys. Rev.* **1933**, *46*, 0618–0622.
- (29) Radom, L.; Schleyer, P. R.; Pople, J. A.; Hehre, W. J. *Ab Initio Molecular Orbital Theory*, 1st ed.; Wiley: New York, 1986.
- (30) Lynch, B.; Truhlar, D. *J. Phys. Chem. A* **2003**, *107*, 3898–3906.
- (31) de Boor, C. *A Practical Guide to Splines*, Rev. ed.; Springer-Verlag: New York, 2001.
- (32) Frisch, M. J.; Trucks, G. W.; Schlegel, H. B.; Scuseria, G. E.; Robb, M. A.; Cheeseman, J. R.; Scalmani, G.; Barone, V.; Mennucci, B.; Petersson, G. A.; Nakatsuji, H.; Caricato, M.; Li, X.; Hratchian, H. P.; Izmaylov, A. F.; Bloino, J.; Zheng, G.; Sonnenberg, J. L.; Hada, M.; Ehara, M.; Toyota, K.; Fukuda, R.; Hasegawa, J.; Ishida, M.; Nakajima, T.; Honda, Y.; Kitao, O.; Nakai, H.; Vreven, T.; Montgomery, J. A., Jr.; Peralta, J. E.; Ogliaro, F.; Bearpark, M.; Heyd, J. J.; Brothers, E.; Kudin, K. N.; Staroverov, V. N.; Kobayashi, R.; Normand, J.; Raghavachari, K.;

Rendell, A.; Burant, J. C.; Iyengar, S. S.; Tomasi, J.; Cossi, M.; Rega, N.; Millam, J. M.; Kleene, M.; Knox, J. E.; Cross, J. B.; Bakken, V.; Adamo, C.; Jaramillo, J.; Gomperts, R.; Stratmann, R. E.; Yazyev, O.; Austin, A. J.; Cammi, R.; Pomelli, C.; Ochterski, J. W.; Martin, R. L.; Morokuma, K.; Zakrzewski, V. G.; Voth, G. A.; Salvador, P.; Dannenberg, J. J.; Dapprich, S.; Daniels, A. D.; Farkas, O.; Foresman, J. B.; Ortiz, J. V.; Cioslowski, J.; Fox, D. J. *Gaussian 09*, Revision A.1; Gaussian, Inc.: Wallingford, CT, 2009.

- (33) Zupan, A.; Perdew, J.; Burke, K. *Int. J. Quantum Chem.* **1997**, *61*, 835–845.
- (34) Zupan, A.; Burke, K.; Emzerhof, M.; Perdew, J. *J. Chem. Phys.* **1997**, *106*, 10184–10193.
- (35) Lacks, D.; Gordon, R. *Phys. Rev. A* **1993**, *47*, 4681–4690.
- (36) Zhang, Y.; Pan, W.; Yang, W. *J. Chem. Phys.* **1997**, *107*, 7921.
- (37) Kannemann, F. O.; Becke, A. D. *J. Chem. Theory Comput.* **2009**, *5*, 719–727.
- (38) Johnson, E. R.; Keinan, S.; Mori-Sanchez, P.; Contreras-Garcia, J.; Cohen, A. J.; Yang, W. *J. Am. Chem. Soc.* **2010**, *132*, 6498–6506.